PHYSICAL REVIEW E VOLUME 60, NUMBER 2 AUGUST 1999

Tensile water transport in a porous gel

Paulo Loureiro de Sousa, M. Engelsberg, and F. G. Brady Moreira
Departamento de Física, Universidade Federal de Pernambuco, 50670-901 Recife-Pernambuco, Brazil
(Received 5 February 1999; revised manuscript received 21 April 1999)

A Monte Carlo simulation model, which incorporates the effect of tensile forces as well as diffusion, is proposed to explain the behavior of water transport in a saturated porous gel. The algorithm is able to account for the puzzling moisture profiles, which were first observed by conventional magnetic resonance imaging and, more recently, by Overhauser imaging. [S1063-651X(99)51208-7]

PACS number(s): 02.70.Lq, 05.40.−a, 76.70.Fz, 76.60.Pc

TENSILE TRANSPORT AND DIFFUSION

Water transport in porous systems is a ubiquitous phenomenon in nature and plays an important role in a variety of processes. Although in many cases a diffusive process obeying Fick's law may furnish an adequate description, there are examples where this behavior may not prevail. In various technologically important processes, Fickian diffusion, with diffusivity generally depending upon local water concentration, has been reported. This appears to be the case for example for drying of cement and plaster [1] and for water uptake in plastics [2,3]. On the other hand, water transport during the drying process of various foods and grains, and in model food gels (MFG) [4,5], appears to exhibit, under special conditions, non-Fickian behavior.

Nuclear magnetic resonance has been used extensively to investigate water transport and self-diffusion in porous systems. Two somewhat different approaches have been employed. Moisture profiles obtained by NMR imaging methods [1–5] have been particularly useful to study water transport on a macroscopic scale, under the influence of external agents. These include concentration gradients caused by drying or externally applied pressure. On the other hand, interpore self-diffusion and its relationship to pore microstructure has been more conveniently studied by pulsed gradient spin echo methods [6–8].

A large enhancement of the NMR signal can be obtained through the Overhauser effect [9]. This involves irradiation of an electron spin resonance transition of a dissolved free radical, prior to data acquisition in the usual NMR imaging mode. The increased sensitivity permits to obtain images even in very low magnetic fields. It has been shown recently [5] that Overhauser imaging [10] in very low magnetic fields may furnish moisture profiles that are extremely sensitive to small variations of local water content. Measurements performed on a MFG, consisting of [4,11] agar, water, and microcrystalline cellulose (MCC) in suitable proportions, have accurately confirmed previous results obtained by conventional NMR imaging in high magnetic fields [4].

Agar is a biopolymer which, in the sol state, is found in the form of random coils. The gelation process is believed to combine these coils into double helices [12], which aggregate into domains separated by relatively large intercommunicating pores. Water molecules can be either free or bound to biopolymer chains and can also exchange at rates which are believed to be fast compared with the NMR transverse relaxation time [12]. Moreover, bound water molecules and protons attached to the biopolymer chains do not contribute to the observable NMR imaging intensity. Given their many applications, agar hydrogels have been studied extensively by various methods [12–15]. Of particular interest for the present work is the addition of MCC to an agar hydrogel. This modifies the pore structure yielding a system with peculiar water transport characteristics [4], which simulates the behavior of food product.

Figure 1 shows a moisture profiles obtained by Overhauser imaging in a cylindrical sample of the MFG as a function of radial distance from the center [5]. Starting from a largely saturated, initially uniform moisture distribution (78% of water and 22% of solids), a sample, 21.4 mm in diameter and 50 mm in height, was exposed to the ambient and allowed to dry laterally in still air. The drying time for the profile shown was 196 min. Also shown in Fig. 1 are numerical solutions $m_w(r,t)/m_w(0)$ of the diffusion equation at $t=196$ min for various values of the diffusion constant. Here, as well as in other simulations, we have assumed

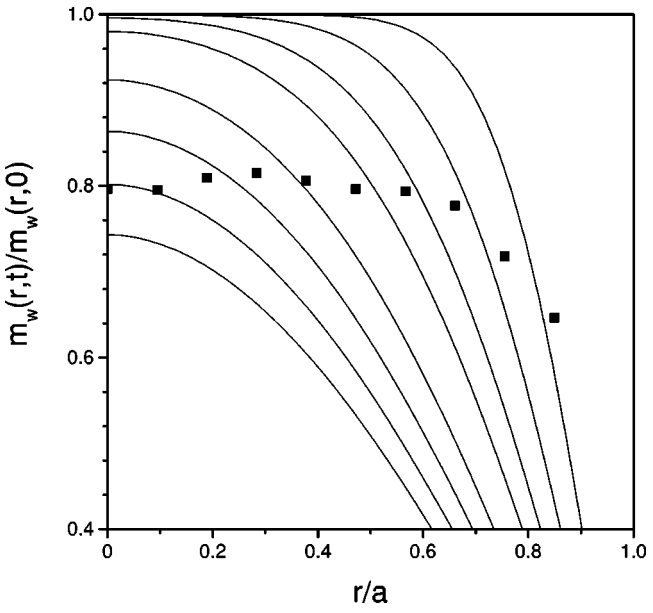

FIG. 1. Numerical solutions of the diffusion equation in a cylinder of radius $a=10.7$ mm for $t=196$ min and various values of the diffusion constant D. From top to bottom $D(10^{-5}$ cm^2/sec$)=0.16$, 0.28, 0.44, 0.59, 0.84, 1.03, 1.21, and 1.38. Also shown (■) is a measured profile at $t=196$ min.

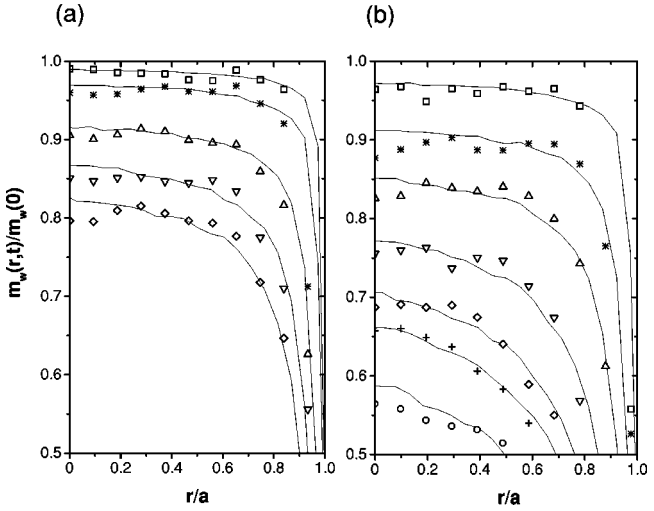

FIG. 2. (a) Measured moisture profiles in a MFG obtained by Overhauser imaging for the following drying times: (□)$t=2$ min, (⋆)$t=15$ min, (△)$t=76$ min, (▽)$t=98$ min, and (◇)$t=176$ min. The solid lines are simulated profiles for the following corresponding numbers of Monte Carlo steps: $N_{mc}=7$, 16, 42, 57, and 114. (b) Measured moisture profiles in a different drying run involving longer times: (□)$t=32$ min, (⋆)$t=53$ min, (△)$t=95$ min, (▽)$t=197$ min, (◇)$t=301$ min, (+)$t=342$ min, and (○)$t=449$ min. The solid lines are simulated profiles for the following corresponding numbers of Monte Carlo steps: $N_{mc}=15$, 44, 73, 138, 194, 230, and 300.

at $r=a$, a boundary condition of constant surface concentration of negligible value. Since we are dealing with the early stages of drying of a largely saturated system this assumption should not greatly affect the results. Figure 1 clearly shows the departure of the measured profile from the Fickian prediction with a constant diffusion coefficient.

Figure 2 shows moisture profiles in the MFG sample for various drying times. The small changes detectable in these profiles, which were obtained in a magnetic field of only 16 mT, underline the large sensitivity to small changes in local moisture attainable by Overhauser imaging. The range of the data shown in Fig. 2 is especially interesting and displays some distinctive features. The moisture contents exhibit well defined plateaus; the amplitudes become appreciably lower as the sample dries but with little change in shape. A similar behavior has, in some cases, also been observed in actual food product [4]. In contrast, for Fickian diffusion with a constant diffusivity, such a drop in the initial amplitude of an initial plateau is accompanied by a marked change to a paraboliclike profile, as shown in Fig. 1. Attempts to infer from profiles such as those of Fig. 2, diffusivities which although not constant, would depend upon concentration alone, were not successful. Hence, a non-Fickian behavior has been postulated for this system [4].

In this Rapid Communication we propose a mechanism, which may be responsible for the peculiar and somewhat puzzling profiles of Fig. 2, as well as a computer simulation algorithm. It includes two different effects. One is diffusion, broadly understood as transport of matter from one part to another resulting from random molecular motion. The other is the effect of tensile forces tending to preserve the integrity of the clusters of fluid, which form within the random network of capillaries.

A familiar phenomenon, illustrating the importance of tensile forces, is the ascending transport of sap through the xylem of trees and plants. The height reached by the water column without breakage, from the roots to the leaves, may by far exceed the maximum height achievable by pulling the water column with a vacuum pump. To explain this phenomenon [16] one has to assume that, under the surface of the leaves, water molecules evaporate one at a time and are individually replaced by molecules pulled from below by surface-tension forces, preserving, in this way, the continuity of the column.

The interplay between diffusion and tensile forces is also important for a description of other phenomena [17] and has been explored extensively by computer simulations using concepts related to invasive percolation [18]. Following somewhat similar lines, we next propose a computer algorithm, which incorporates, at least some aspects, of the complex phenomenology of the problem and allows a description of the peculiar moisture profiles revealed by NMR imaging.

SIMULATIONS

The proposed algorithm employs a two-dimensional square lattice with an inscribed circular boundary of constant radius to simulate a long cylindrical sample. In reality, the radius of a MFG sample is not constant but actually slightly shrinks, by approximately 10%, in the range of drying times of Fig. 2(b) [5].

Each lattice site may be thought to represent a pore and fluid is allowed to diffuse to neighboring pores along capillaries represented by the ''bonds'' between the given site and its nearest neighbors. Diffusers occupying sites linked by nearest neighbors bonds define a cluster. Given the spatial resolution of the NMR images a square lattice of 40×40 sites was found to be adequate for our purpose. The $N=1600$ sites forming the lattice are initially randomly filled with M diffusers, and one of the sites within the inscribed circle is randomly chosen as well as one of its nearest neighbors. We first consider purely diffusive motion. In this case, if the chosen lattice site is occupied by a diffuser and the chosen neighbor is empty, the diffuser will jump to the empty site independently of the occupation of other sites. If the chosen lattice site is empty or the chosen neighbor is occupied, a new random choice is performed. Moreover, if a jump occurs, the position of the diffuser is actualized and a new draw is made. Thus, after the process has been repeated N times, each diffuser has attempted, on the average, one jump and Monte Carlo time is incremented by one unit.

External drying conditions are simulated in the algorithm by introducing a probability p_s for a diffuser to be removed from the lattice when it reaches the boundary. Each ''pixel'' in a simulation furnishes the average occupation number over a large number n_r of repetitions. For a radial profile parallel to a lattice direction, since $\sqrt{N}$ is an even number, we averaged the occupation number of the two adjacent sites equidistant from the center line to define a pixel. The average occupation number of a pixel, at a given Monte Carlo time, is proportional to the concentration of fluid $m_w(r,t)$ at the given radial distance and time.

As a check of the algorithm, profiles obtained with a number of repetitions, varying between $n_r=4\times10^5$ and n_r

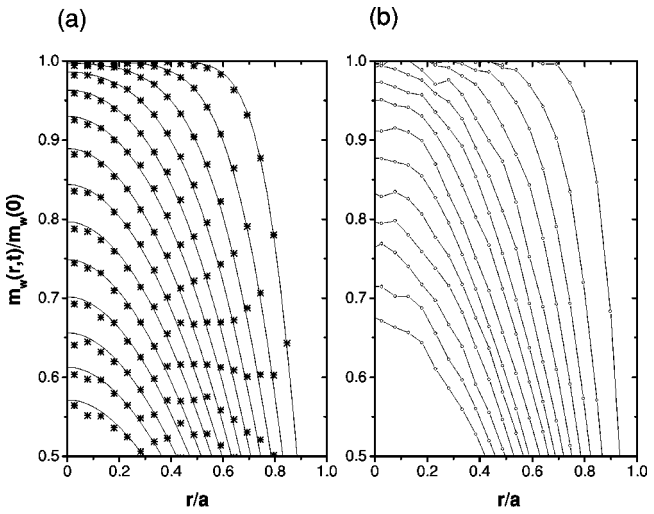

FIG. 3. (a) Calculated profiles (solid lines) using a numerical solution of the diffusion equation with a constant diffusivity D, and initial uniform distribution $m_w(0)$. The adimensional time Dt/a^2 is incremented from top to bottom in steps of 0.0125. Computer simulations ($\star$) of the corresponding purely diffusive profiles. For $N=1600$, N_{mc} is incremented from top to bottom in steps of 20. The number of Monte Carlo steps in each profile is related to the adimensional time through $N_{mc}/N=Dt/a^2$. (b) Computer simulations of tensile transport profiles for $M/N=0.05$ and $N=1600$. The number of Monte Carlo steps N_{mc} in the algorithm is increased from top to bottom in increments of 20. The lines are only a guide to the eye.

$=10^7$ (for the case of very small values of M/N), were compared with a numerical solution of the diffusion equation for a cylinder of radius a and constant diffusivity D [19]. Denoting by N_{mc} the number of Monte Carlo steps, the ratio time, N_{mc}/N, in the simulation, should correspond to the actual adimensional time, Dt/a^2, in the numerical solution. The radial distance was expressed in units of the total number of radial pixels in the simulation, and in units of a in the numerical solution.

Figure 3(a) shows numerical solutions of the diffusion equation and Monte Carlo profiles, at the corresponding times $Dt/a^2=N_{mc}/N$. An evaporation probability $p_s=1$ was assumed in the Monte Carlo profiles, with an initial condition corresponding to a uniform radial distribution of diffusers $m_w(0)$. As expected, the agreement is very good. Moreover, the profiles of Fig. 3(a) appear to be in sharp contrast with the experimental data of Fig. 2.

In order to take into account tensile effects, we next propose the following modification of the above transport algorithm. After one site and a nearest neighbor have been randomly chosen among the N lattice sites, and assuming the first to be occupied and the second empty, the diffuser will jump to the empty site, but now its motion may affect the position of other diffusers belonging to the same cluster. For relatively high concentration of diffusers, each site left vacant by the motion of a member of the cluster is filled by another nearest neighbor diffuser, thus preserving the integrity of the aggregates. When several diffusers may jump into the same site, a random choice with equal probability is employed to avoid conflict. Moreover, Monte Carlo time is advanced one unit after N random choices just as in the case of purely diffusive motion.

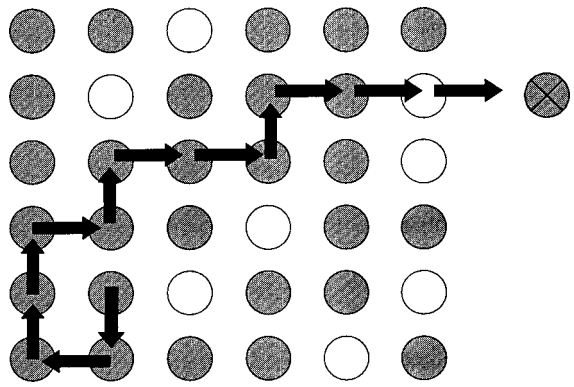

FIG. 4. Schematic representation of the tensile transport algorithm. A surface diffuser ($\times$) evaporates leaving a vacancy which is filled causing a collective motion within a cluster.

As before, a diffuser reaching a site on the boundary may be removed with probability p_s. However, if it evaporates, the vacancy will be filled by a randomly chosen nearest neighbor diffuser. The process is iterated until the vacancy created, either reaches a dead end or all its nearest neighbors have already participated in the collective motion. Similarly, when a diffuser belonging to a cluster jumps to an empty site in the bulk, the same collective motion from randomly chosen sites to the site left vacant is performed. Figure 4 schematically shows some details of the algorithm. Because of the presence of tensile forces, the probability of a jump for a given diffuser, either at the surface or in the bulk, is assumed to depend upon the occupation of its nearest neighbors. If an occupied site with an empty neighboring site is surrounded, for example, by three filled sites, the diffuser is assumed to be tightly bound and a low probability, denoted by $p(3)$, is

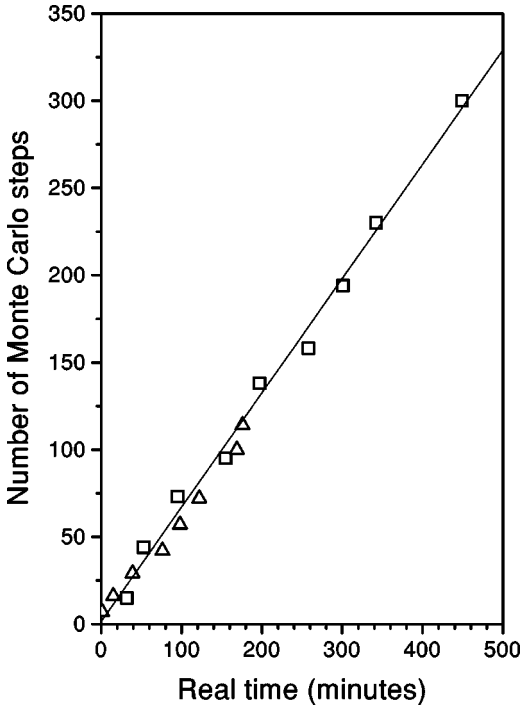

FIG. 5. Number of Monte Carlo steps N_{mc} as a function of real drying times for the simulated and experimental profiles of Fig. 2. Obtained from the profiles of Figs. 2(a) ($\triangle$) and from the 2(b) ($\square$).

assigned. On the contrary, if the occupied site is surrounded by empty sites, the corresponding probability $p(0)$ is a maximum.

Unlike simple diffusion with a constant diffusivity, the profiles in our tensile transport model depend upon the initial concentration of diffusers M/N, which is one of the adjustable parameters of the model. The other adjustable parameter is the ratio of probabilities $\lambda = p(3)/p(1) = p(2)/p(0)$, which we assumed to be equal for both bulk jumping as well as surface removal. For simplicity and, to keep the number of adjustable parameters at a minimum, we have also considered $p(1) \sim p(0) = 1$ and $p(3) \sim p(2) = \lambda$. Figure 2 shows simulated profiles for various Monte Carlo times with $\lambda = 0.2$ and a value of $M/N = 0.98$ close to saturation. The agreement appears to be quite satisfactory. Although the two parameters defined above are sufficient to simulate the profiles in the limited range of moisture content of Fig. 2, it is conceivable that a probability for breakage of a cluster during the collective, reptationlike motion [20] may exist [16] and could become appreciable for lower concentrations. If one assumes, for example, a value of 0.1 for this probability of breakage and, furthermore, that it only affects members of the collective motion with a coordination number of 1, one obtains profiles such as those shown in Fig. 3(b). As expected, the inclusion of such a small breakage probability does not affect appreciably the profiles for values of M/N close to unity. However, it yields profiles that become progressively paraboliclike as the initial moisture content is decreased. For the case shown in Fig. 3(b), corresponding to an initial concentration $M/N = 0.05$, they appear to converge asymptotically to the simple Fickian limit of Fig. 3(a).

It is also quite instructive to obtain a relation between Monte Carlo time and a physical time. Figure 5 shows a plot of Monte Carlo time N_{mc} as a function of real time for the simulated and experimental profiles of Fig. 2. For simple diffusion with a constant diffusivity D, one expects a ratio $N_{mc}/t = ND/a^2$. For our tensile transport model, the slope of the straight line of Fig. 5 yields a value $N_{mc}a^2/tN = 0.62 \times 10^{-5}$ cm^2/sec, which could be likewise interpreted as an effective global diffusivity. In spite of the non-Fickian character of the transport process in this MFG, suggested by the NMR imaging profiles, global diffusivity values determined, for example, by desorption measurements are often quoted [11]. From desorption measurements performed in our sample we found a value of 0.57×10^{-5} cm^2/sec, in reasonable agreement with the above result.

A Monte Carlo algorithm for Fickian diffusion has been modified to include tensile effects. The interplay between random motion and tensile forces, which tend to preserve the integrity of clusters of diffusers, appears to be essential to explain the experimental profiles of Fig. 2. Although our transport model could be made more realistic, it should be applicable, even in its present relatively simple form, in a description of water transport in porous gels as revealed by NMR imaging, with its inherent space and time scales.

ACKNOWLEDGMENTS

We wish to thank L.A. Colnago and B. Stošić for assistance. This work was supported by Conselho Nacional de Desenvolvimento Científico e Tecnológico and Financiadora de Estudos e Projetos (Brazilian agencies).

[1] R. J. Gummerson, C. Hall, W. D. Hoff, R. Hawkes, G. N. Holland, and W. S. Moore, Nature (London) **281**, 56 (1979).
[2] S. Blackband and P. Mansfield, J. Phys. C **19**, L49 (1986).
[3] P. Mansfield, R. Bowtell, and S. Blackband, J. Magn. Reson. **99**, 507 (1992).
[4] G. W. Schrader and J. B. Litchfield, Dry. Technol. **10**, 295 (1992).
[5] P. L. de Sousa, M. Engelsberg, M. A. Matos, and L. A. Colnago, Meas. Sci. Technol. **9**, 1982 (1998).
[6] P. T. Callaghan, A. Coy, T. P. J. Halpin, D. Mac Gowan, K. J. Packer, and F. O. Zelaya, J. Chem. Phys. **97**, 651 (1992).
[7] P. T. Callaghan and A. Coy, Phys. Rev. Lett. **68**, 3176 (1992).
[8] S. Matsukawa and I. Ando, Macromolecules **30**, 8310 (1997).
[9] W. Overhauser, Phys. Rev. **92**, 411 (1953).
[10] D. J. Lurie, in *Encyclopedia of Nuclear Magnetic Resonance*, edited by D. M. Grant and R. K. Harris (Wiley, New York, 1995).
[11] B. Biquet and T. P. Labuza, J. Food Proc. Pres. **12**, 151 (1988).
[12] P. S. Belton, B. P. Hills, and E. R. Raimbaud, Mol. Phys. **63**, 825 (1988).
[13] I. Mrani, G. Fras, and J. C. Bénet, J. Phys. III **5**, 985 (1995).
[14] M. M. Chui, R. J. Phillips, and M. J. McCarthy, J. Colloid Interface Sci. **174**, 336 (1995).
[15] H. D. Middendorf, Physica B **226**, 113 (1996).
[16] M. H. Zimmermann, *Xylem Structure and the Ascent of Sap* (Springer-Verlag, Berlin, 1988); see also Sci. Am. **208**, 133 (1963).
[17] S. Crestana and A. N. D. Posadas, in *Fractals in Soil Science*, edited by P. Baveye, J. Y. Parlange, and B. A. Stewart (CRC Press, Boca Raton, FL, 1998).
[18] D. Wilkinson and J. F. Willemsen, J. Phys. A **16**, 3365 (1983).
[19] J. Crank, *The Mathematics of Diffusion*, 2nd ed. (Oxford University Press, London, 1975).
[20] P. G. de Gennes, J. Chem. Phys. **55**, 572 (1971).